



Published in final edited form as:

Mol Cancer Res. 2022 May 04; 20(5): 699–711. doi:10.1158/1541-7786.MCR-21-0837.

Inactivation of p21-Activated Kinase 2 (Pak2) Inhibits the Development of *Nf2*-Deficient Tumors by Restricting Downstream Hedgehog and Wnt Signaling

Eleonora Sementino^{1,*}, Yuwaraj Kadariya^{1,*}, Mitchell Cheung¹, Craig W. Menges¹, Yinfei Tan², Anna-Mariya Kukuyan¹, Ujjawal Shrestha¹, Sofiia Karchugina¹, Kathy Q. Cai³, Suraj Peri⁴, James S. Duncan¹, Jonathan Chernoff¹, Joseph R. Testa^{1,#}

¹Cancer Signaling and Epigenetics Program, Fox Chase Cancer Center, Philadelphia, Pennsylvania.

²Genomics Facility, Fox Chase Cancer Center, Philadelphia, Pennsylvania.

³Histopathology Facility, Fox Chase Cancer Center, Philadelphia, Pennsylvania.

⁴Bioinformatics and Biostatistics Facility, Fox Chase Cancer Center, Philadelphia, Pennsylvania.

Abstract

Since loss of the *NF2* tumor suppressor gene results in p21-activated kinase (Pak) activation, PAK inhibitors hold promise for the treatment of *NF2*-deficient tumors. To test this possibility, we asked if loss of *Pak2*, a highly expressed group I PAK member, affects the development of malignant mesothelioma in *Nf2*;*Cdkn2a*-deficient (*NC*) mice and the growth properties of *NC* mesothelioma cells in culture. *In vivo*, deletion of *Pak2* resulted in a markedly decreased incidence and delayed onset of both pleural and peritoneal malignant mesotheliomas in *NC* mice. *In vitro*, *Pak2* deletion decreased malignant mesothelioma cell viability, migration, clonogenicity, and spheroid formation. RNA-seq analysis demonstrated downregulated expression of Hedgehog and Wnt pathway genes in *NC*;*Pak2*^{-/-} mesothelioma cells versus *NC*;*Pak2*^{+/+} mesothelioma cells. Targeting of the Hedgehog signaling component Gli1 or its target gene *Myc* inhibited cell viability and spheroid formation in *NC*;*P*^{+/+} mesothelioma cells. Kinome profiling uncovered kinase changes indicative of EMT in *NC*;*Pak2*^{-/-} mesothelioma cells, suggesting that *Pak2*-deficient malignant mesotheliomas can adapt by reprogramming their kinome in the absence of Pak activity. The identification of such compensatory pathways offers opportunities for rational combination therapies to circumvent resistance to anti-PAK drugs.

Keywords

Conditional knockout mice; malignant mesothelioma; *Nf2* and *Cdkn2a* tumor suppressor genes; PAK; Hedgehog and Wnt signaling; cancer stem cells

#Joseph R. Testa, Ph.D., Fox Chase Cancer Center, 333 Cottman Avenue, Philadelphia, PA 19111; Phone: (215) 728-2610; Fax: (215) 214-1619; joseph.testa@fccc.edu.

*These authors contributed equally to this work.

Conflict of Interest Statement

JRT has provided legal consultation regarding genetic aspects of mesothelioma. The remaining authors have no potential conflicts of interest with regard to the publication of this work.

Introduction

Malignant mesotheliomas are medically unresponsive cancers that arise mainly from the serosal membranes lining the pleural and peritoneal cavities. Most (85%) mesotheliomas arise in the pleura, but about 10%–20% of cases develop from the peritoneal surfaces (1). Malignant mesotheliomas often occur after chronic exposure of mesothelial cells to asbestos fibers (2). Malignant mesothelioma causes more than 3,000 deaths annually in the U.S., and a significant increase in mesothelioma incidence is predicted in certain developing countries where asbestos usage is increasing at an alarming rate and where protection of workers is minimal.

Although pleural and peritoneal mesotheliomas exhibit some genomic differences, both are characterized by frequent somatic loss/inactivation of certain tumor suppressor genes, prominent among them being *BAP1*, *NF2*, and *CDKN2A/B* (3–14). *NF2* mutations and loss of expression of the *NF2* product, Merlin, have been reported in up to ~55% of mesothelioma cell lines (6). Among pleural mesotheliomas characterized in The Cancer Genome Atlas (TCGA) database, monoallelic deletions of *NF2* were observed in ~35% of samples and biallelic inactivation in another 40% of tumors, with many of the latter harboring mutations of one allele (12). In peritoneal mesothelioma, mutations and allelic losses of *NF2* have been observed in 21%–35% of cases (11,13,14). Underscoring the relevance of *NF2* inactivation to mesothelioma pathogenesis, heterozygous *Nf2* knockout mice treated with asbestos develop mesothelioma at a significantly higher frequency and markedly accelerated rate than their wild-type counterparts (7,15). Moreover, in one of these studies, 9/9 mesothelioma cell lines established from neoplastic ascites from asbestos-exposed *Nf2*^{+/-} mice exhibited loss of the wild-type *Nf2* allele, and expression of Merlin was consistently absent in these cells (7).

Merlin has been implicated in various tumor-related signaling pathways, prominent among them being p21-activated kinase (PAK) and Hippo signaling. Merlin regulates the protein kinases Mst1 and Mst2 (mammalian sterile 20-like 1 and -2; *a.k.a.* serine/threonine protein kinase Stk4 and Stk3) and the serine/threonine kinases Lats1 and -2 (large tumor suppressor 1 and -2). Merlin and each of these kinases are components of the highly conserved Hippo signaling pathway, which regulates organ size in *Drosophila* and mammals. Combined Mst1/2 deficiency in the liver results in loss of inhibitory phosphorylation of the downstream oncoprotein Yap1 and development of hepatocellular carcinoma (16). *Nf2*-deficient phenotypes in multiple tissues were suppressed by heterozygous deletion of *Yap1*, suggesting that Yap is a major effector of Merlin in growth regulation. The Hippo tumor-suppressive signaling pathway has also been connected with Merlin-deficient mesothelioma (17,18). Other work has shown that Merlin suppresses tumorigenesis by activating upstream components of the Hippo pathway by inhibiting the E3 ubiquitin ligase CRL4(DCAF1) (19).

Merlin is regulated by phosphorylation, with hypophosphorylated Merlin being the growth-inhibitory, functionally active tumor suppressor form, whereas hyperphosphorylated Merlin is growth-permissive (20,21). PAK directly phosphorylates Merlin at serine residue 518, a site that regulates Merlin activity and localization (22,23). Such phosphorylation of

Merlin weakens its head-to-tail self-association and its association with the cytoskeleton (24). Furthermore, functional analysis of serine 518 phosphorylation has demonstrated that expression of a phospho-mimic mutant (Merlin S518D) caused striking changes in cell proliferation and shape, stimulating the creation of filopodia (25). These results strongly suggest that Merlin's growth and motility suppression functions are attenuated following phosphorylation by PAK. Moreover, it is noteworthy that many mesotheliomas that lack *NF2* mutations nevertheless show functional inactivation of Merlin via constitutive phosphorylation of Ser518, in some cases as a result of inhibition of a Merlin phosphatase (26).

PAKs are serine/threonine protein kinases that are binding partners for the small GTPases Cdc42 and Rac, and they represent one of the most highly conserved effector proteins for these enzymes (27). Mammalian tissues contain six PAK isoforms: group I (Pak1, -2, and -3) and group 2 (Pak4, -5, and -6). These two groups differ substantially in form, function and tissue expression, with only group I PAKs appearing to be involved in Merlin signaling (28). Group I PAKs, in particular Pak1, have oncogenic properties when expressed at high levels. In most settings, expression of PAK1 stimulates cell proliferation, survival, and motility (28,29). Group I PAKs are frequently activated in human malignant mesotheliomas, and genetic or pharmacologic inhibition of PAKs is sufficient to inhibit mesothelioma cell proliferation and survival (30). Importantly, Merlin is more than just a target for PAK; it is also a negative regulator of this kinase. Merlin binds to and inactivates Pak1, and loss of Merlin results in the activation of Pak1 (24). These results suggest that the growth and motility abnormalities of *NF2*-null cells might in part be attributed to the activation of PAK and its downstream targets. These data also suggest that inhibitors of PAK might be useful in switching off such signaling pathways.

We hypothesized that loss of PAK activity would counteract some aspects of *NF2*/Merlin loss-of-function by compromising key downstream oncogenic signaling pathways in mesothelial cells. To test this possibility, we crossed *Nf2^{fl/fl};Cdkn2a^{fl/fl}* mice to mice with conditional deletion of *Pak2*, which encodes the most highly expressed group I PAK isoform in most tissues. Cohorts of these animals were then injected in either the pleural or peritoneal cavities with adeno-Cre virus to delete floxed alleles in the mesothelial lining, with the goal being to determine if *Pak2* loss diminishes tumor onset and/or progression at one or both sites where mesothelioma typically originates. We show that loss of *Pak2* indeed delays mesothelioma tumorigenesis, though studies employing multiplexed kinase inhibitor beads and mass spectrometry (MIB/MS) and RNA-seq technologies revealed that these mesothelioma cells ultimately reprogram their kinome in the absence of Pak2 activity. The identification of such secondary pathways offers opportunities for the rational design of combination therapies to circumvent resistance to anti-PAK drugs.

Materials and Methods

Mouse strains

LucR;Nf2^{fl/fl};Cdkna^{fl/fl} mice (31), a kind gift of Dr. Anton Berns, and *Pak2^{fl/fl}* mice (32), were maintained in a mixed FVB/N × 129/Sv background. All studies were performed in accordance with protocol #18-03 approved by the Fox Chase Cancer Center (FCCC)

Institutional Animal Care and Use Committee (IACUC). The specific primer sequences for the genotyping are listed in Supplementary Table S1. All PCR were at $T_a = 58^\circ\text{C}$ for 30 cycles.

Adeno-Cre injections, tumor collection, and mesothelioma cell line generation

For studies involving intrathoracic (IT) and intraperitoneal (i.p.) injections of Ad5CMVCre (adeno-Cre) virus, animals with $Nf2^{f/f};Cdkn2a^{f/f};Pak2^{+/+}$ and $Nf2^{f/f};Cdkn2a^{f/f};Pak2^{f/f}$ genotypes were divided into two cohorts with equivalent numbers of male and female mice in each group. At 8–10 weeks of age, mice were injected either IT or i.p. with adeno-Cre virus (50 μl of $3\text{--}6 \times 10^{10}$ PFU) in PBS. Expression of adeno-Cre results in the removal of the floxed exons in the *Nf2*, *Cdkn2a*, and *Pak2* loci, generating the following genotypes in infected cells: $Nf2^{-/-};Cdkn2a^{-/-}$ and $Nf2^{-/-};Cdkn2a^{-/-};Pak2^{-/-}$, and the resulting malignant mesotheliomas are referred to as $NC;P^{+/+}$ and $NC;P^{-/-}$ tumors hereafter. All mice were monitored daily for tumor formation for up to 12 months. Mice were sacrificed by CO_2 inhalation upon signs of pain/distress or illness as judged by lethargic behavior, weight loss or bloating, difficulty in breathing, hunched posture, rough hair coat, dehydration or detectable tumor volume approaching 10% of overall body weight. Tissues of all organs of both cavities were collected from sacrificed mice, and tumor specimens were subjected to histopathological assessment by an experienced animal pathologist (K.Q.C.) of FCCC's Histopathology Facility. Portions of tumors were saved in RNAlater Solution (Thermo Fisher Scientific, Waltham, MA) and frozen at -80°C for subsequent study. When possible, a portion of the fresh primary tumor was also chopped into fine pieces and incubated with 0.2% collagenase for 2 h and then cultured in DMEM supplemented with 10% FCS (GIBCO) and penicillin/streptomycin (GIBCO). The minced tissues were grown at 37°C in 5% CO_2 for 2–3 d. Cells that attached to culture dishes and grew out were passaged to establish cell lines. Once the pathologist confirmed by H&E and IHC that the corresponding primary tumor was diagnosed as a mesothelioma, we validated that the derived cell line expressed mesothelioma markers, e.g., WT1 and mesothelin, by semi-quantitative PCR and/or immunoblotting. All mesothelioma cell lines were tested for mycoplasma regularly using LookOut® Mycoplasma PCR Detection Kit (Millipore Sigma, # MP0035-1KT) up until the last experiments were performed. Thawing of the cell lines for experiments was typically at passage 3, and all experiments were conducted using the earliest passages possible (p4–p5), with no experiments performed beyond passage 6.

Detection of tumors and statistical considerations

Survival curves for $NC;P^{+/+}$ versus $NC;P^{-/-}$ mice were compared using one-sided, log-rank tests. Kaplan-Meier plots were used to display time to tumor detection among the two separate cohorts for both IT and i.p. injection studies.

Tumor histopathology/immunohistochemistry

Histopathology and immunohistochemistry of malignant mesothelioma tissues were performed according to our usual method (33).

Preparation of luciferin and *in vivo* bioluminescent imaging (BLI)

LucR:Nf2^{fl/fl};Cdkn2a^{fl/fl} mice were crossed to *Pak2^{fl/fl}* mice to generate offspring with different *Pak2* genotypes ($^{+/+}$, $^{+/f}$, $^{f/f}$), which at 8–10 weeks of age were injected IT with adeno-Cre virus. Beginning at 6–7 weeks after virus injections, littermates with different genotypes were injected i.p. with 150 mg of filtered *D-Luciferin*, Firefly, potassium salt (Caliper Life Sciences) in PBS per kg mouse body weight 10 min before imaging. The Cre recombinase removes a floxed polyadenylation acid sequence before the ORF of the luciferase reporter transgene (*LucR*) permitting luciferase expression for monitoring tumor progression. BLI scans were acquired using an IVIS Spectrum Imaging System (Caliper Life Sciences) as described (34) to assess the presence and relative size of tumors, as indicated by the intensity of luminescent signals detected. The same mice were imaged weekly until tumors began to form. The experiment was repeated four times.

Preparation of lentivirus expressing shRNA against *Pak2* and infection of *NC;P^{+/+}* mesothelioma cells

A Tet-pLKO-puro plasmid was a gift from Dmitri Wiederschain (Addgene, plasmid # 21915). The shRNAs targeting mouse *Pak2* were created by the cloning of annealed forward and reverse oligos synthesized based on information provided at the Broad Institute's website (<https://portals.broadinstitute.org/gpp/public/>). Lentivirus was produced by cotransfecting into HEK293T cells separately Tet-inducible sh*Pak2* #70, sh*Pak2* #85, and sh*GFP* with psPAX2 and pMD2.G plasmids using lipofectamine 2000 (Thermo Fisher Scientific). After 24 h and 48 h, virus particles were collected, filtered and then used to infect cell lines for the *in vivo* experiment described below. For a second set of experiments, lentivirus was produced by transfecting 293T cells with the three separate pLKO sh*Pak2* or with control sh*GFP*. Lentivirus particles harboring the three different sh*Pak2* constructs or control sh*GFP* were used to infect peritoneal *NC;P^{+/+}* MM cell lines. Cells were seeded in 6-well plates and infected with virus particles containing polybrene (sc-134220; Santa Cruz) at a concentration of 2 $\mu\text{g}/\text{ml}$, centrifuged at 2,000 rpm for 2 h, and incubated in a humidified 5% CO₂ incubator at 37°C for 24 h. The following day, supernatant was removed and cells were selected with puromycin (4 $\mu\text{g}/\text{mL}$) and then used for immunoblotting and cell viability, clonogenicity, and spheroids assays. The clone numbers and target sequences for sh*Pak2* are shown in Supplementary Table S1.

In vivo model to assess lung tumor burden of mesothelioma cells following doxycycline-inducible shRNA knockdown of *Pak2*

In this experiment, we used tumor cell line (MM87) derived from an asbestos-induced mesothelioma seen in a *Nf2^{+/-};Cdkn2a^{+/-}* mouse (35). Stable MM87 cells expressing tet-inducible lentiviruses against *Pak2* (sh*Pak2* #70 and #85) were injected into the tail vein of three NSG mice (0.5×10^6 cells/mouse), followed by i.p. administration of doxycycline beginning after d 7 and then every 2 d thereafter. Animals were sacrificed on d 21, and then the lungs were harvested for histopathological assessment of tumor colonization using an *Aperio* ScanScope CS2 scanner (*Aperio*, Vista, CA) (see Supplementary Materials and Methods for details).

Preparation of lentivirus expressing *Pak2* and infection of *NC;P^{-/-}* mesothelioma cell lines

Preparation and infection of *NC;P^{-/-}* mesothelioma cells with untagged *Pak2*, HA-tagged *Pak2*, and control pLenti were performed using the same protocol described above (see Supplementary Materials and Methods for details). After selection was completed, the cells were used for immunoblotting as well as cell viability and clonogenicity assays.

Immunoblot analysis and antibodies

For immunoblotting, protein lysates were prepared as previously described (35). Lysates (30-50 µg/sample) were loaded on gels, transferred to nitrocellulose membranes (1620115, Bio-Rad, Hercules, CA), and probed with primary antibodies listed in Supplementary Table S2. Anti-rabbit secondary antibody (45-000-682, 1:5000) and anti-mouse secondary antibody (45-000-679, 1:5000-50000 depending on the primary antibody) were from Fisher Scientific (Waltham, MA). Immunoblots were imaged using Immobilon Western Chemiluminescent HRP Substrate (ECL) (WBKLS0500, MilliporeSigma, Ontario Canada).

Cell fractionation studies

Cell fractionation of *NC;P^{-/-}* and *NC;P^{+/+}* peritoneal mesothelioma cell lines was performed using a Protease Inhibitor Cocktail (#11836170001, MilliporeSigma), as described in the Supplementary Materials and Methods. For immunoblotting, protein lysates were prepared as previously described (35).

Migration assay

In vitro migration of *NC;P^{-/-}* and *NC;P^{+/+}* mesothelioma cell lines was determined using a Transwell Multiwell Plate with Polyester Membrane Inserts (Corning, Edison, NJ), following the manufacturer's protocol. The migrating cells on the underside of the membrane were fixed and stained with a Diff-Quik stain kit (Siemens).

Cell viability and clonogenic assays

NC;P^{+/+} cell lines with stable knockdown of *Pak2* were trypsinized, counted, and seeded in 96-well plates at 500 cells/well. In a different experiment *NC;P^{+/+}* and *NC;P^{-/-}* cell lines were seeded in 96-well plates (2,500 cells/well), and 24 h after seeding, the cells were treated with the indicated concentrations of GANT61 (in medium containing 2.5% FBS) and either JQ1 or DMSO (the latter two with 10% FBS) for 72–96 h. Cell viability was determined was assessed using a CellTiter 96 AQueous One Solution Cell Proliferation Assay (MTS) (G3582; Promega, Madison, WI), according to the manufacturer's instructions. The same protocol was used to perform a cell viability assay involving the stable overexpression of *Pak2* in *NC;P^{-/-}* cells.

Clonogenic assays were performed by seeding *NC;P^{+/+}* cell lines with stable knockdown of *Pak2* in triplicate in 10-cm Petri dishes at a density of 10,000 cells/dish. Colonies were stained and counted after 2 weeks, using a Diff-Quik stain kit (Siemens). Each experiment was performed in triplicate. For quantification of the clonogenic assay, each stained 10-cm dish was incubated in a shaker with 6 ml of 0.01N HCL for 15 min. Then 100 µl of solution was transferred in 96-well plates, and the absorbance was determined at 630 nm.

The same protocol was used to perform a clonogenic assay for stable overexpression of Pak2 in *NC;P^{-/-}* cells.

Spheroid formation assay

Spheroid formation in *NC;P^{-/-}* and *NC;P^{+/+}* mesothelioma cell lines were performed using ultra-low attachment 6-well plates (5,000 cells/well, Corning #3471) in serum-free DMEM/F12 medium supplemented with B27, EGF (10 ng/mL), mouse basic FGF (10 ng/mL) and penicillin/streptomycin. Spheroids were photographed after 10 d of cell culture. Mesothelioma cell lines were incubated with or without drug (GANT61, a Gli1 inhibitor, or JQ1, an inhibitor of bromodomain proteins, one of which (BRD4) regulates Myc transcription) for 10 d, and then spheroids were photographed.

RNA-seq and gene set enrichment analyses performed on peritoneal primary mesotheliomas

RNA was isolated from *NC;P^{+/+}* and *NC;P^{-/-}* primary peritoneal mesotheliomas using TRIzol (Thermo Fisher Scientific) and purified using RNeasy columns (Qiagen, Germantown, MD) following the manufacturers' instructions. The RNA quality was determined using a Bioanalyzer (Agilent). RNA-seq analysis was performed on a set of tumors (5 primary *NC;P^{-/-}* mesotheliomas and 3 primary *NC;P^{+/+}* mesotheliomas) by Novogene (Sacramento, CA), using its Illumina NovoSeq 6000 platform. Raw sequence counts for each gene were produced with HTseq (<https://htseq.readthedocs.io>), and differentially expressed genes were determined using DESeq2 (36). For functional enrichment analysis, genes identified as differentially expressed with nominal p-value < 0.5 were ranked by fold-change and mapped to human genes using R biomaRt (37), and these genes were analyzed using the GSEA Preranked method of Gene Set Enrichment Analysis (GSEA) (38). Further details are shown in the extended Supplementary Materials and Methods. Raw sequencing data have been deposited in the GEO repository with the dataset Series record GSE192660.

Semi-quantitative reverse transcriptase PCR analysis

For semiquantitative reverse transcriptase PCR (RT-PCR) analysis, 1 µg of total mRNA was retrotranscribed into cDNA from a subset of *NC;P^{-/-}* and *NC;P^{+/+}* primary peritoneal tumors and cell lines. Normal mesothelial cell cultures (NMC) were used as controls. Reverse transcription was performed using SuperScript II Reverse Transcriptase (Thermo Fisher Scientific) following the manufacturer's protocol. RT-PCR analysis was performed to confirm the diagnosis of malignant mesothelioma and to validate RNA sequencing experiments. PCR was performed using REDTaq (Sigma) with the annealing temperature at 58°C. PCR products were run on 2% ethidium bromide gels. The primer sequences are shown in Supplementary Tables S1 (mesothelioma marker genes) and S3 (differentially expressed genes).

MIBs preparation and chromatography

To gain an unbiased and more comprehensive view of Merlin signaling, kinome reprogramming analysis was performed using MIB/MS (39). In brief, cells were lysed on

ice in buffer containing 50 mM HEPES (pH 7.5), 0.5% Triton X-100, 150 mM NaCl, 1 mM EDTA, 1 mM EGTA, 10 mM sodium fluoride, 2.5 mM sodium orthovanadate, 1X protease inhibitor cocktail (Roche), and 1% each of phosphatase inhibitor cocktails 2 and 3 (Sigma). Particulate was removed by centrifuging lysates at 21,000 g for 15 min at 4°C and filtering through 0.45 µm syringe filters. Protein concentrations were determined by BCA analysis (Thermo Fisher Scientific). Endogenous kinases were isolated by flowing lysates over kinase inhibitor-conjugated Sepharose beads (purvalanol B, VI16832, PP58 and CTx-0294885 beads) in 10 ml gravity-flow columns. After 2×10-ml column washes in high-salt buffer and 1×10-ml wash in low-salt buffer (50 mM HEPES, pH 7.5), 0.5% Triton X-100, 1 mM EDTA, 1 mM EGTA, 10 mM sodium fluoride, and 1M NaCl or 150 mM NaCl, respectively, retained kinases were eluted from the column by boiling in 2 × 500 µl of 0.5% SDS, 0.1 M TrisHCl (pH 6.8), and 1% 2-mercaptoethanol. Eluted peptides were reduced by incubation with 5 mM DTT at 65°C for 25 min, alkylated with 20 mM iodoacetamide at room temperature for 30 min in the dark, and alkylation was quenched with DTT for 10 min. Samples were concentrated to ~100 µl with Millipore 10-kD cutoff spin concentrators. Detergent was removed by chloroform/methanol extraction, and the protein pellet was resuspended in 50 mM ammonium bicarbonate and digested with sequencing-grade modified trypsin (Promega) overnight at 37°C. Peptides were cleaned with PepClean C18 spin columns (Thermo Fisher), dried in a speed-vac, resuspended in 50 µl of 0.1% formic acid, extracted with ethyl acetate (10:1 ethyl acetate:H₂O), washed five times in 1 mL ethyl acetate, and then dried in a speed vac. Nano-LC-MS/MS and data processing for the kinome profiling analysis were performed as described in detail elsewhere (40). The mass spectrometry proteomics data have been deposited to the ProteomeXchange Consortium via the PRIDE partner repository with the dataset identifier PXD030571.

Results

Inactivation of *Pak2* results in decreased incidence and delayed onset and progression of pleural and peritoneal mesotheliomas in *Nf2*-deficient mice

Locotemporal expression of Cre recombinase by either IT or i.p. injection of adeno-Cre virus was used to induce mesothelial cell-specific homozygous deletions of *Nf2*, *Cdkn2a*, with or without excision of *Pak2*, in homozygous compound CKO mice. Examples of genotyping of *Nf2^{fl/fl};Cdkn2a^{fl/fl};Pak2^{+/+}* and *Nf2^{fl/fl};Cdkn2a^{fl/fl};Pak2^{fl/fl}* mice and immunoblotting demonstrating loss of expression of conditionally knocked out genes in malignant mesotheliomas arising after injection of adeno-Cre virus are depicted in Fig. 1A and 1B, respectively. The IT-injected mice were followed for up to 1 year, and by the end of the study, 16/19 *NC;P^{+/+}* animals (84%) developed pleural mesothelioma, with a median survival of 26 weeks. In contrast, only 8/15 (53%) *NC;P^{-/-}* mice developed pleural mesothelioma, and the median survival was prolonged to 34 weeks. Among animals injected i.p. with adeno-Cre virus, 18/22 (82%) *NC;P^{+/+}* mice developed peritoneal mesothelioma (median survival: 24 weeks) versus only 10/23 (43%) *NC;P^{-/-}* mice (median survival: 35 weeks). Malignant mesothelioma incidence and Kaplan-Meier survival curves of IT- and i.p.-injected mice that developed mesothelioma are shown in Figure 1C and 1D, respectively. In both the IT and the i.p. studies, the incidence of mesothelioma was much lower in *NC;P^{-/-}* mice than in the *NC;P^{+/+}* cohort. Statistical differences in survivals of *NC;P^{+/+}*

versus *NC;P^{-/-}* mice with mesothelioma were highly significant in both IT and i.p. studies. Mesotheliomas from *NC;P^{+/+}* and *NC;P^{-/-}* mice showed similar histopathology, with the vast majority of tumors in both the pleural and peritoneal models being sarcomatoid (Supplemental Figure S1), which is consistent with our previous studies of mesotheliomas in conditional *NC* mice (33). No purely epithelioid tumors were observed. Several were biphasic, with a predominance of spindle cells.

Generally, the pleural mesotheliomas were solitary and more massive than the tumors observed in the peritoneum. In pleural mesotheliomas, there was no obvious overall tumor size difference between *Pak2* WT and *Pak2* KO tumors. Moreover, we were able to generate tumor cell lines from a high percentage of the pleural tumors, regardless of the *Pak2* status. Mesotheliomas in the peritoneum typically presented as multiple, diffuse, small nodules that often caused intestinal obstructions. Notably, *Pak2* loss in peritoneal mesotheliomas resulted in diminished tumor size and multiplicity. Also, while ~80% of *Pak2* WT tumors formed cell lines, <20% of *Pak2* KO tumors did so.

In vivo bioluminescent imaging confirms that loss of *Pak2* delays malignant mesothelioma progression in *Nf2*-deficient mice

BLI scanning revealed intense luminescent signals in *NC;P^{+/+}* mice beginning at about 6 months, with less signal observed in *NC;P^{+/-}* (heterozygous loss of *Pak2*) littermates (Figure 1E). BLI scanning was repeated with four sets of littermates with different *Pak2* genotypes, and in each instance tumor progression, as indicated by diminished intensity of the luminescent signals observed, was consistently delayed in mice with homozygous excision of *Pak2*.

Knockdown of *Pak2* diminishes metastatic colonization of *Nf2*-deficient malignant mesothelioma cells in the lung

Malignant mesothelioma cells (MM87), which were previously derived from an asbestos exposed *Nf2^{+/-};Cdkn2a^{+/-}* mouse, were infected with tet-inducible lentiviruses against *Pak2*. Two clones that demonstrated marked knockdown of *Pak2* (sh*Pak2* #85 and sh*Pak2* #70 in Figure 2A) were expanded and injected individually into the tail vein of NSG mice. The mice were injected with doxycycline i.p. after 7 d, when the tumors have become established, and then every 2 d thereafter; all animals were sacrificed on d 21, and lungs were examined histopathologically for tumor colonization (Figure 2B). H&E staining revealed that tumor colonization of the lungs by MM87 cells was consistently diminished in the cell clones expressing shRNA against *Pak2* versus control MM87 cells infected with lentivirus expressing shRNA against *GFP* (Figure 2C), and the differences were statistically significant ($p < 0.05$).

Deletion of *Pak2* results in decreased tumor cell migration

We compared cell migration of pleural mesothelioma cells from *NC;P^{+/+}* mice versus mesothelioma cells from *NC;P^{-/-}* mice. Twenty-two hours after seeding, the cells were evaluated for migratory ability using a transwell migration assay, as described in the Materials and Methods. As shown in Supplemental Figure S2, a pleural *NC;P^{-/-}*

mesothelioma cell line tested showed markedly less migration than a *NC;P^{+/+}* mesothelioma cell line.

***Pak2* loss results in diminished mesothelioma cell viability, clonogenicity, and spheroid formation**

The *NC;P^{+/+}* peritoneal mesothelioma cell lines tested formed large spheroids when seeded in ultra-low attachment 6-well plates in stem cell media, whereas the *NC;P^{-/-}* peritoneal mesothelioma lines did not (Fig. 3A). Stable knockdown of *Pak2* with lentivirus expressing three separate shRNA (sh*Pak2* #12, #70, and #85), which was confirmed by immunoblotting (Fig. 3B), was shown to inhibit cell viability in two different *NC;P^{+/+}* mesothelioma cell lines, as assessed by MTS assay (Fig. 3C). Furthermore, stable knockdown of *Pak2* caused a marked reduction in spheroid formation in *NC;P^{+/+}* cell lines (Fig. 3D). Clonogenicity was also decreased by stable *Pak2* knockdown in *NC;P^{+/+}* cells (Fig. 3E). Reciprocally, re-expression of *Pak2* in *NC;P^{-/-}* cell lines resulted in increases in both cell viability and clonogenicity (Supplemental Figure S3).

RNA-seq analysis reveals that *Pak2* loss in *Cdkn2a;Nf2*-null primary mesotheliomas leads to diminished expression of genes involved in oncogenic pathways

RNA-seq analysis was performed on 3 primary *NC;P^{+/+}* peritoneal mesotheliomas and 5 primary *NC;P^{-/-}* peritoneal mesotheliomas to identify genes that are differentially expressed due to loss of *Pak2*, one of the main downstream effectors of *Nf2*. Most differentially expressed genes in the *NC;P^{-/-}* tumors were downregulated. Many of the downregulated genes are involved in muscle contraction and cardiac epithelial-mesenchymal transition (EMT) pathways (Supplemental Figure S4), whereas others are involved in Wnt (*Wif1*, *Axin2*, *Gli1*, *Gpc3*, *Sfrp5*, *Fzd4/8/9*, *Lrp4*, *Wnt9b*) and Hedgehog (*Gli1*) signaling. Other downregulated genes involved kinase and other cancer-related pathways (*Igf2*, *Fgfr3/4*, *Notch3*, *Hey1*, *Tgfb2*, and *Ifi44l*), stem cell markers (*Sox8/11*), and integrins (*Itga7/8*). Fewer upregulated genes were observed in the *NC;P^{-/-}* mesotheliomas; these included a Wnt inhibitor gene (*Dkk2*), a gene encoding a kinase (*Styk1*), and a transcription repressor gene (*Foxg1*). A heatmap of genes differentially expressed in *NC;P^{-/-}* mesotheliomas versus *NC;P^{+/+}* mesotheliomas is shown in Figure 4, including genes involved in Wnt and Hedgehog signaling (Figure 4A) and various other pathways (Figure 4B). Multiple cancer-related genes validated by semi-quantitative RT-PCR analysis are shown in Figure 4C along with several mesothelial markers such as *Wt1* and *Msln* (mesothelin). Immunoblot analysis of *Nf2*/Merlin, *Pak2*, p16Ink4a, and p19Arf in 3 *NC;P^{-/-}* and 3 *NC;P^{+/+}* primary peritoneal mesotheliomas corresponding to a subset of the tumors used for the RNA-seq analysis are shown in Figure 4D.

***Pak2* loss in malignant mesothelioma results in downregulated Hedgehog and Wnt signaling and diminished cancer stem cell (CSC) properties**

Semi-quantitative PCR analysis was also performed on early passage *NC;P^{-/-}* and *NC;P^{+/+}* peritoneal mesothelioma cell lines. These studies confirmed that *NC;P^{-/-}* cells exhibited down regulation of genes involved in Hedgehog signaling (*Gli1*, *Gli2*), CSCs (*Sox2*, *Nanog*, *Nes*), cell migration/invasion (*Adam8*, *Mmp9*), and Wnt signaling (*Lrp4*, *Lrg6*, *Wnt10b*, *Stmn2*) (Fig. 5A). Immunoblotting of *NC;P^{-/-}* and *NC;P^{+/+}* cell lines demonstrated loss of

expression of Pak2, Nf2, p16Ink4a, p19Arf and Myc, an activator and transcriptional target of Hedgehog signaling, in *NC;P^{-/-}* cells (Fig. 5B). Cell fractionation studies of the *NC;P^{-/-}* and *NC;P^{+/+}* peritoneal mesothelioma cell lines were performed, and immunoblot analysis revealed decreased nuclear expression of Gli1 and Myc in *NC;P^{-/-}* cells (Fig. 5C).

Assessment of kinome reprogramming in *Pak2*-null pleural mesothelioma cells using MIB/MS technology

Given that the development of drug resistance is a significant factor in aggressive tumors such as malignant mesothelioma, we also used a technological approach, MIB/MS, that globally measures kinase signaling at the proteomic level (39,40) to assess dynamic reprogramming of the kinome in response to genetic inhibition of *Pak2* in malignant mesothelioma. This technology was used to compare the kinase expression of an early passage *NC;P^{+/+}* pleural mesothelioma cell line with that of an early passage *NC;P^{-/-}* pleural mesothelioma line, with studies performed in triplicate. Kinome activity, principal component analysis (PCA), identities of up- and down-regulated kinases, and heat-map are depicted in Figure 6A–D. The kinome profiling revealed that as compared to *NC;P^{+/+}* mesothelioma cells, *NC;P^{-/-}* mesothelioma cells had multiple kinase changes suggestive of EMT. Prominent among the changes associated with *Pak2* loss were up regulation of *Pdgfra*, *Pdgfrβ*, *Limk1*, *Fyn*, *Jak1* and *Mkk6* along with down regulation of *Ddr1*. Immunoblot confirmation of expression changes in selected kinases is shown in Figure 6E, with upregulated expression of *Pdgfra*, *Pdgfrβ*, and phospho-Stat3 being consistently observed in multiple *NC;P^{-/-}* cell lines versus *NC;P^{+/+}* lines (Fig. 6F).

Targeting of Gli1 or Myc inhibits cell viability and spheroid formation in *NC;P^{+/+}* mesothelioma cells

Early passage *NC;P^{-/-}* and *NC;P^{+/+}* peritoneal mesothelioma cell lines were seeded in 96-well plates and treated with various concentrations of GANT61, a Gli1/2 inhibitor, and JQ1, an inhibitor of bromodomain proteins, one of which (BRD4) regulates *Myc* transcription. MTS assays demonstrated substantial decreases in cell viability in *NC;P^{+/+}* cells compared to *NC;P^{-/-}* cells at higher concentrations of GANT61 and JQ1 (Fig. 7A). Moreover, both GANT61 and JQ1 radically inhibited the formation of spheroids in *NC;P^{+/+}* cells, whereas little effect was observed with either drug in *NC;P^{-/-}* cells (Fig. 7B). Semi-quantitative PCR analysis (Fig. 7C) of the *NC;P^{+/+}* cells demonstrated that GANT61 decreased the expression of *Gli1* mRNA expression at a concentration of 5 μM, which was also the concentration that effectively inhibited spheroid formation (Fig. 7B). Immunoblot analysis demonstrated the JQ1 diminished the expression of *Myc* at 39 and 78 nM (Fig. 7D), doses that were also sufficient to markedly inhibit spheroid formation. However, we acknowledge that JQ1 has activity against several other targets besides BRD4, including other BET proteins, and we did not examine directly whether the effects we observed are mediated via BRD4.

Discussion

Losses of *NF2* and *CDKN2A* are thought to play a critical role in malignant mesothelioma pathogenesis. In fact, in human peritoneal mesothelioma, homozygous deletions in *CDKN2A* and hemizygous loss of *NF2* as detected by fluorescence *in situ* hybridization has

been reported to confer a poor clinical outcome, whereas loss of *BAP1* was not associated with clinical outcome (11). In conditional knockout mice, *Nf2^{fl/fl}* mice and *Cdkn2a^{fl/fl}* mice injected IT with adeno-Cre virus resulted in very few pleural mesotheliomas, whereas *Nf2^{fl/fl};Cdkn2a^{fl/fl}* mice injected with adeno-Cre virus resulted in aggressive thoracic tumor growth (31,33). In the present study, *Nf2^{fl/fl};Cdkn2a^{fl/fl};Pak2^{fl/fl}* mice acquire loss of only a single Group I PAK gene in the mesothelial lining following injection with adeno-Cre virus; yet, this was sufficient to significantly decrease the incidence and delay the onset and progression of both pleural and peritoneal mesotheliomas when compared to that of *NC* mice retaining *Pak2*.

Group I PAKs are frequently activated in human malignant mesotheliomas, and genetic or pharmacologic inhibition of PAKs is sufficient to inhibit mesothelioma cell proliferation and survival (30). Pak1 is frequently overexpressed in human breast, ovarian, bladder and brain cancers, often secondary to amplification of its 11q13.5–14 chromosomal locus (41). Moreover, breast and bladder carcinoma cells bearing such amplification were shown to be highly sensitive to PAK inhibition by small molecule inhibitors or RNAi, suggesting that these cancer cells are “addicted” to Pak1 overexpression. The role of Pak2 in human neoplasia is less well studied, but it has been linked to a variety of human cancers (27). The pathways that mediate the oncogenic effects of PAK overexpression are not fully known, but include activation of the Erk pathway (via phosphorylation of Raf and Mek), inactivation of *NF2*/Merlin, stabilization of β -catenin, and possibly scaffolding interactions that link Pdk1 with Akt (27). Loss of PAK function is associated with decreased cell proliferation and motility, with concomitant loss of activity of these signaling pathways (42,43). Consistent with these data, we demonstrate that loss of *Pak2* results in diminished mesothelioma cell migration and downregulated expression of two genes, *Adam8* and *Mmp9*, that have been implicated in cell migration and invasion. Additionally, other *in vitro* studies revealed that loss of Pak2 in mesothelioma cells results in decreased cell viability, clonogenicity, and spheroid formation.

Pak1 and Pak2, while similar in sequence and structure, nevertheless have a number of distinct functions. For example, although both isoforms are broadly expressed, deletion of the *Pak2* gene in mice leads to early embryonic lethality, whereas deletion of *Pak1* has little effect on development, longevity, or fertility (27). Further, cardiovascular toxicity of anti-PAK small molecule inhibitors are related to blockade of PAK2 rather than PAK1 (44). The mechanistic bases for these differences are not yet well understood, but may be related to differences in intracellular locations and/or intrinsic differences in substrate preferences (27). These distinguishing features need to be kept in mind when considering potential therapeutic interventions.

Our RNA-seq analysis demonstrated that loss of Pak2 counteracts some aspects of *Nf2* loss-of-function in mesothelioma cells by downregulating the expression of multiple genes involved in oncogenic pathways, particularly genes encoding proteins involved in Hedgehog (Gli1/2) and Wnt signaling. In response to activation of Hedgehog signaling, Gli proteins are processed into transcriptional activators that induce expression of target genes, including *Myc*, *Nanog*, *Sox2* and *Wnt*, all genes that are downregulated in *NC;P^{-/-}* versus *NC;P^{+/+}* cells. Notably, the CSC marker genes *Sox2*, *Nanog* and *Nes* (nestin), a new putative marker

of CSCs (45), were all upregulated in *NC;P^{+/+}* cells, which correlates with the prominent spheroid formation properties observed in these cells. Germane to this, we have previously reported cooperativity between *Nf2* and *Cdkn2a* losses to drive the development of highly aggressive mesotheliomas characterized by large tumor spheroids in ascites, enhanced tumor spreading capability, and the presence of a CSC population (35).

Collectively, the findings presented here point to a positive role for group I PAKs in tumorigenesis mediated by several central signaling pathways, Hedgehog and Wnt being prominent among them. Our findings further suggest that inhibitors of PAK might be useful in switching off such signaling pathways. Furthermore, these data help establish a framework for understanding malignant mesothelioma adaptation and permit the design of rational combinations of targeted agents, as clinical or near-clinical inhibitors for many protein kinases already exist.

We found that targeting of Gli1 or Myc, two activators and effectors of Hedgehog signaling, inhibited cell viability and spheroid formation in *NC;P^{+/+}* mesothelioma cells but had minimal effect on NC cells with loss of Pak2. Similarly, in studies of primary colorectal cancer organoid cultures, treatment with GANT61 inhibited expression of stem cell markers such as Myc and Nanog, which was thought to occur via decreased transcription of *GLI1* (46). GLI1 is a transcriptional effector at the terminus of the Hedgehog pathway, and in certain cancers, aberrant activation of the Hedgehog pathway has been shown to promote dedifferentiation to a more stem-like phenotype (47).

The RNA-seq profiling presented here also demonstrated that numerous genes that are downregulated in *NC;P^{-/-}* mesothelioma cells are involved in muscle contraction and cardiac EMT pathways. These data are consistent with previous work showing a significant role for Group I PAKs in myoblast and cardiac muscle function. For example, the Rac1-Pak2 pathway has been shown to be indispensable for zebrafish heart regeneration (48). In addition, Group I PAKs have been shown to promote skeletal myoblast differentiation during postnatal development and regeneration in mice, and adult mice conditionally lacking both *Pak1* and *Pak2* in the skeletal muscle lineage developed an age-related myopathy, with muscles exhibiting centrally-nucleated myofibers, fibrosis, and signs of degeneration (49). As in the RNA-seq studies, kinome profiling assayed by MIB/MS technology also uncovered kinase changes indicative of EMT in *NC;P^{-/-}* mesothelioma cells, including up regulation of *Pdgfra*, *Pdgfrβ* and *Fyn* kinases, as well as up regulation of the EMT transcription regulator *Slug*. Recent work has clarified the EMT cell plasticity program as a set of dynamic transitional states between the epithelial and mesenchymal phenotypes, with EMT and its intermediary states serving as critical drivers of organ fibrosis and tumor progression (50). The upregulation of these genes in *NC;P^{-/-}* mesothelioma cells may represent an adaptive survival mechanism that can be rationally targeted to prevent the emergence of resistance to PAK small molecule inhibitors.

Collectively, the findings presented here suggest that *Nf2*-deficient mesothelioma cells with loss of Pak2 ultimately adapt by reprogramming their kinome and transcriptome in the absence of PAK activity. While PAKs are vital to oncogenic signaling in *NF2*-null mesothelioma cells, targeted genetic inactivation of *Pak2* in *Nf2*-null mesothelioma cells

resulted in downregulated expression of genes involved in oncogenic pathways. Eventually, however, malignant mesotheliomas develop in *NC;P^{-/-}* mice apparently by compensatory activation of oncogenic pathways involving other kinases such as *Styk1*, *Pdgfra/β*, *Jak/Stat* and *Fyn*, as well as by gene expression changes such as downregulation of the tumor suppressor gene *If44il* and upregulation of *Dkk2*. Such information can inform the design of rational combination therapies for malignant mesothelioma using molecularly targeted inhibitors. The identification of such secondary pathways that could be co-targeted to prevent resistance to anti-PAK drugs thus sets the stage for future preclinical studies with novel therapeutics.

Supplementary Material

Refer to Web version on PubMed Central for supplementary material.

Acknowledgments

This work was supported by NCI grants CA148805 (to J.R. Testa and J. Chernoff) and CA06927 (to FCCC) and an appropriation from the Commonwealth of Pennsylvania to FCCC. Other support was provided by the Local #14 Mesothelioma Fund of the International Association of Heat and Frost Insulators and Allied Workers. The authors thank Michael Slifker and Dr. Alison M. Kurimchak for compiling and depositing datasets in the GEO repository and ProteomeXchange, respectively. The following FCCC core services assisted this project: Laboratory Animal, Transgenic Mouse, Genomics, Cell Culture, Histopathology, and Biostatistics and Bioinformatics Facilities.

References

- Kindler HL. Peritoneal mesothelioma: the site of origin matters. *Am Soc Clin Oncol Educ Book* 2013;33:182–8.
- Britton M The epidemiology of mesothelioma. *Semin Oncol* 2002;29:18–25.
- Cheng JQ, Jhanwar SC, Klein WM, Bell DW, Lee W-C, Altomare DA, et al. p16 alterations and deletion mapping of 9p21-p22 in malignant mesothelioma. *Cancer Res* 1994;54:5547–51. [PubMed: 7923195]
- Sekido Y, Pass HI, Bader S, Mew DJY, Christman MF, Gazdar AF, et al. Neurofibromatosis type 2 (*NF2*) gene is somatically mutated in mesothelioma but not in lung cancer. *Cancer Res* 1995;55:1227–31. [PubMed: 7882313]
- Bianchi AB, Mitsunaga S-I, Cheng JQ, Klein WM, Jhanwar SC, Seizinger B, et al. High frequency of inactivating mutations in the neurofibromatosis type 2 gene (*NF2*) in primary malignant mesotheliomas. *Proc Natl Acad Sci U S A* 1995;92:10854–8. [PubMed: 7479897]
- Cheng JQ, Lee WC, Klein MA, Cheng GZ, Jhanwar SC, Testa JR. Frequent mutations of *NF2* and allelic loss from chromosome band 22q12 in malignant mesothelioma: evidence for a two-hit mechanism of *NF2* inactivation. *Genes Chromosomes Cancer* 1999;24:238–42. [PubMed: 10451704]
- Altomare DA, Vaslet CA, Skele KL, De Rienzo A, Devarajan K, Jhanwar SC, et al. A mouse model recapitulating molecular features of human mesothelioma. *Cancer Res* 2005;65:8090–5. [PubMed: 16166281]
- Bott M, Brevet M, Taylor BS, Shimizu S, Ito T, Wang L, et al. The nuclear deubiquitinase BAP1 is commonly inactivated by somatic mutations and 3p21.1 losses in malignant pleural mesothelioma. *Nat Genet* 2011;43:668–72. [PubMed: 21642991]
- Testa JR, Cheung M, Pei J, Below JE, Tan Y, Sementino E, et al. Germline *BAP1* mutations predispose to malignant mesothelioma. *Nat Genet* 2011;43:1022–5. [PubMed: 21874000]
- Nasu M, Emi M, Pastorino S, Tanji M, Powers A, Luk H, et al. High incidence of somatic *BAP1* alterations in sporadic malignant mesothelioma. *J Thorac Oncol* 2015;10:565–76. [PubMed: 25658628]

11. Singhi AD, Krasinskas AM, Choudry HA, Bartlett DL, Pingpank JF, Zeh HJ, et al. The prognostic significance of *BAP1*, *NF2*, and *CDKN2A* in malignant peritoneal mesothelioma. *Mod Pathol* 2016;29:14–24. [PubMed: 26493618]
12. Hmeljak J, Sanchez-Vega F, Hoadley KA, Shih J, Stewart C, Heiman D, et al. Integrative molecular characterization of malignant pleural mesothelioma. *Cancer Discov* 2018;8:1548–65. [PubMed: 30322867]
13. Hung YP, Dong F, Torre M, Crum CP, Bueno R, Chirieac LR. Molecular characterization of diffuse malignant peritoneal mesothelioma. *Mod Pathol* 2020;33:2269–79. [PubMed: 32504035]
14. Offin M, Yang SR, Egger J, Jayakumaran G, Spencer RS, Lopardo J, et al. Molecular characterization of peritoneal mesotheliomas. *J Thorac Oncol* 2021;Oct 11;S1556–0864(21)03215–9. doi: 10.1016/j.jtho.2021.09.012. Online ahead of print
15. Fleury-Feith J, Lecomte C, Renier A, Matrat M, Kheuang L, Abramowski V, et al. Hemizyosity of *Nf2* is associated with increased susceptibility to asbestos-induced peritoneal tumours. *Oncogene* 2003;22:3799–805. [PubMed: 12802287]
16. Zhou D, Conrad C, Xia F, Park JS, Payer B, Yin Y, et al. Mst1 and Mst2 maintain hepatocyte quiescence and suppress hepatocellular carcinoma development through inactivation of the *Yap1* oncogene. *Cancer Cell* 2009;16:425–38. [PubMed: 19878874]
17. Murakami H, Mizuno T, Taniguchi T, Fujii M, Ishiguro F, Fukui T, et al. *LATS2* is a tumor suppressor gene of malignant mesothelioma. *Cancer Res* 2011;71:873–83. [PubMed: 21245096]
18. Mizuno T, Murakami H, Fujii M, Ishiguro F, Tanaka I, Kondo Y, et al. YAP induces malignant mesothelioma cell proliferation by upregulating transcription of cell cycle-promoting genes. *Oncogene* 2012;31:5117–22. [PubMed: 22286761]
19. Li W, Cooper J, Zhou L, Yang C, Erdjument-Bromage H, Zagzag D, et al. Merlin/NF2 loss-driven tumorigenesis linked to CRL4(DCAF1)-mediated inhibition of the hippo pathway kinases Lats1 and 2 in the nucleus. *Cancer Cell* 2014;26:48–60. [PubMed: 25026211]
20. Shaw RJ, McClatchey AI, Jacks T. Localization and functional domains of the neurofibromatosis type II tumor suppressor, merlin. *Cell Growth Diff* 1998;9:287–96. [PubMed: 9563848]
21. Morrison H, Sherman LS, Legg J, Banine F, Isacke C, Haiepek CA, et al. The *NF2* tumor suppressor gene product, merlin, mediates contact inhibition of growth through interactions with CD44. *Genes Dev* 2001;15:968–80. [PubMed: 11316791]
22. Xiao GH, Beeser A, Chernoff J, Testa JR. p21-activated kinase links Rac/Cdc42 signaling to merlin. *J Biol Chem* 2002;277:883–6. [PubMed: 11719502]
23. Kissil JL, Johnson KC, Eckman MS, Jacks T. Merlin phosphorylation by p21-activated kinase 2 and effects of phosphorylation on merlin localization. *J Biol Chem* 2002;277:10394–9. [PubMed: 11782491]
24. Kissil JL, Wilker EW, Johnson KC, Eckman MS, Yaffe MB, Jacks T. Merlin, the product of the *Nf2* tumor suppressor gene, is an inhibitor of the p21-activated kinase, Pak1. *Mol Cell* 2003;12:841–9. [PubMed: 14580336]
25. Rong R, Surace EI, Haiepek CA, Gutmann DH, Ye K. Serine 518 phosphorylation modulates merlin intramolecular association and binding to critical effectors important for NF2 growth suppression. *Oncogene* 2004;23:8447–54. [PubMed: 15378014]
26. Thurneysen C, Opitz I, Kurtz S, Weder W, Stahel RA, Felley-Bosco E. Functional inactivation of NF2/merlin in human mesothelioma. *Lung Cancer* 2009;64:140–7. [PubMed: 18835652]
27. Radu M, Semenova G, Kosoff R, Chernoff J. PAK signalling during the development and progression of cancer. *Nat Rev Cancer* 2014;14:13–25. [PubMed: 24505617]
28. Hofmann C, Shepelev M, Chernoff J. The genetics of Pak. *J Cell Sci* 2004;117:4343–54. [PubMed: 15331659]
29. Bokoch GM. Biology of the p21-activated kinases. *Annu Rev Biochem* 2003;72:743–81. [PubMed: 12676796]
30. Menges CW, Sementino E, Talarchek J, Xu J, Chernoff J, Peterson JR, et al. Group I p21-activated kinases (PAKs) promote tumor cell proliferation and survival through the AKT1 and Raf-MAPK pathways. *Mol Cancer Res* 2012;10:1178–88. [PubMed: 22798428]
31. Jongsma J, van Montfort E, Vooijs M, Zevenhoven J, Krimpenfort P, van der Valk M, et al. A conditional mouse model for malignant mesothelioma. *Cancer Cell* 2008;12:261–71.

32. Radu M, Lyle K, Hoeflich KP, Villamar-Cruz O, Koeppen H, Chernoff J. p21-activated kinase 2 regulates endothelial development and function through the Bmk1/Erk5 pathway. *Mol Cell Biol* 2015;35:3990–4005. [PubMed: 26391956]
33. Kukuyan AM, Sementino E, Kadariya Y, Menges CW, Cheung M, Tan Y, et al. Inactivation of *Bap1* cooperates with losses of *Nf2* and *Cdkn2a* to drive the development of pleural malignant mesothelioma in conditional mouse models. *Cancer Res* 2019;79:4113–23. [PubMed: 31151962]
34. Connolly DC, Hensley HH. Xenograft and transgenic mouse models of epithelial ovarian cancer and non-invasive imaging modalities to monitor ovarian tumor growth *in situ*: applications in evaluating novel therapeutic agents. *Curr Protoc Pharmacol* 2009;45:14.2.1–2.6. [PubMed: 20634901]
35. Menges CW, Kadariya Y, Altomare D, Talarchek J, Neumann-Domer E, Wu Y, et al. Tumor suppressor alterations cooperate to drive aggressive mesotheliomas with enriched cancer stem cells via a p53-miR-34a-c-Met axis. *Cancer Res* 2014;74:1261–71. [PubMed: 24371224]
36. Love MI, Huber W, Anders S. Moderated estimation of fold change and dispersion for RNA-seq data with DESeq2. *Genome Biol* 2014;15:550. [PubMed: 25516281]
37. Durinck S, Spellman PT, Birney E, Huber W. Mapping identifiers for the integration of genomic datasets with the R/Bioconductor package biomaRt. *Nat Protoc* 2009;4:1184–91. [PubMed: 19617889]
38. Subramanian A, Tamayo P, Mootha VK, Mukherjee S, Ebert BL, Gillette MA, et al. Gene set enrichment analysis: a knowledge-based approach for interpreting genome-wide expression profiles. *Proc Natl Acad Sci U S A* 2005;102:15545–50. [PubMed: 16199517]
39. Kurimchak AM, Shelton C, Duncan KE, Johnson KJ, Brown J, O'Brien S, et al. Resistance to BET bromodomain inhibitors is mediated by kinome reprogramming in ovarian cancer. *Cell Rep* 2016;16:1273–86. [PubMed: 27452461]
40. Kurimchak AM, Kumar V, Herrera-Montávez C, Johnson KJ, Srivastava N, Devarajan K, et al. Kinome profiling of primary endometrial tumors using multiplexed inhibitor beads and mass spectrometry identifies SRPK1 as candidate therapeutic target. *Mol Cell Proteomics* 2020;19:2068–90. [PubMed: 32994315]
41. Dummler B, Ohshiro K, Kumar R, Field J. Pak protein kinases and their role in cancer. *Cancer Metastasis Rev* 2009;28:51–63. [PubMed: 19165420]
42. Sells MA, Boyd JT, Chernoff J. p21-activated kinase 1 (Pak1) regulates cell motility in mammalian fibroblasts. *J Cell Biol* 1999;145:837–49. [PubMed: 10330410]
43. Allen JD, Jaffer ZM, Park SJ, Burgin S, Hofmann C, Sells MA, et al. p21-activated kinase regulates mast cell degranulation via effects on calcium mobilization and cytoskeletal dynamics. *Blood* 2009;113:2695–705. [PubMed: 19124833]
44. Rudolph J, Murray LJ, Ndubaku CO, O'Brien T, Blackwood E, Wang W, et al. Chemically diverse group I p21-activated kinase (PAK) inhibitors impart acute cardiovascular toxicity with a narrow therapeutic window. *J Med Chem* 2016;59:5520–41. [PubMed: 27167326]
45. Neradil J, Veselska R. Nestin as a marker of cancer stem cells. *Cancer Sci* 2015;106:803–11. [PubMed: 25940879]
46. Usui T, Sakurai M, Umata K, Elbadawy M, Ohama T, Yamawaki H, et al. Hedgehog signals mediate anti-cancer drug resistance in three-dimensional primary colorectal cancer organoid culture. *Int J Mol Sci* 2018;19:1098.
47. Avery JT, Zhang R, Boohaker RJ. GLI1: A Therapeutic target for cancer. *Front Oncol* 2021;11:673154. [PubMed: 34113570]
48. Peng X, He Q, Li G, Ma J, Zhong TP. Rac1-PAK2 pathway Is essential for zebrafish heart regeneration. *Biochem Biophys Res Commun* 2016;472:637–42. [PubMed: 26966072]
49. Joseph GA, Hung M, Goel AJ, Hong M, Rieder MK, Beckmann ND, et al. Late-onset megaconial myopathy in mice lacking group I Paks. *Skelet Muscle* 2019;9:5. [PubMed: 30791960]
50. Nieto MA, Huang RY-J, Jackson RA, Thiery JP. EMT: 2016. *Cell* 2016;166:21–45. [PubMed: 27368099]

Implications

We provide evidence supporting a role for PAK inhibitors in treating NF2-deficient tumors. NF2-deficient tumors lacking Pak2 eventually adapt by kinome reprogramming, presenting opportunities for combination therapies to bypass anti-PAK drug resistance.

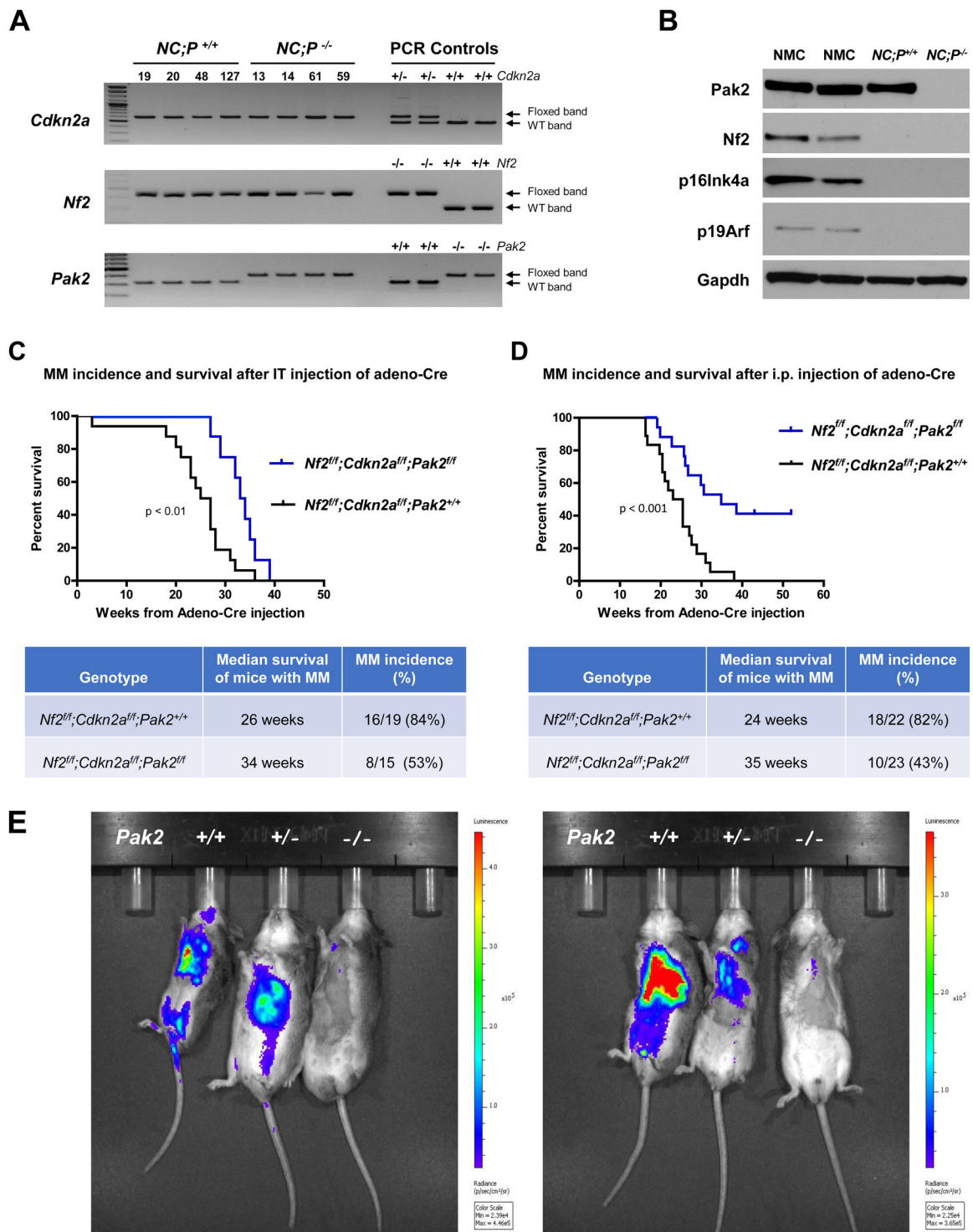


Figure 1. Genotyping and characterization of mesothelioma development in, *Nf2^{fl/fl};Cdkn2a^{fl/fl};Pak2^{+/+}* and *Nf2^{fl/fl};Cdkn2a^{fl/fl};Pak2^{fl/fl}* mice injected intrathoracically or intraperitoneally with adeno-Cre virus. (A) Genotyping of tail DNA from four representative *Nf2^{fl/fl};Cdkn2a^{fl/fl};Pak2^{+/+}* mice and four *Nf2^{fl/fl};Cdkn2a^{fl/fl};Pak2^{fl/fl}* mice that developed peritoneal mesothelioma.

PCR controls for floxed and wild type alleles of *Cdkn2a*, *Nf2* and *Pak2* were from tail DNA of heterozygous and homozygous conditional knockout mice. **(B)** Immunoblotting of two early passage cell lines derived from *NC;P^{-/-}* and *NC;P^{+/+}* peritoneal mesotheliomas demonstrating loss of expression of conditionally knocked out genes in tumor cells. NMC, normal mesothelial cells. **(C, D)** Malignant mesothelioma progression, incidence and Kaplan-Meier survival curves of cohorts of *Nf2^{fl/fl};Cdkna^{fl/fl};Pak2^{+/+}* and *Nf2^{fl/fl};Cdkna^{fl/fl};Pak2^{fl/fl}* mice injected intrathoracically **(C)** or intraperitoneally **(D)** with adeno-Cre virus and succumbing to mesothelioma. Abbreviations: IT, intrathoracic (injection); i.p., intraperitoneal (injection); MM, malignant mesothelioma. **(E)** Bioluminescent imaging reveals delayed mesothelioma progression in mice with *Nf2*-null mesothelial lining and excision of one or both alleles of *Pak2*. *flLucR;Nf2^{fl/fl};Cdkn2a^{fl/fl}* mice were crossed to *Pak2^{fl/fl}* mice to generate offspring having wild type (^{+/+}) *Pak2* or with one or both floxed (^{+/fl} or ^{fl/fl}, respectively) *Pak2* alleles. Mice were injected IT with adeno-Cre virus to excise floxed alleles of thoracic mesothelial lining cells. Infection with adeno-Cre virus also removes a floxed polyadenylation sequence before the ORF of a luciferase reporter transgene (*LucR*). The latter permits luciferase expression to monitor tumor progression, using *D-luciferin* as a substrate and bioluminescent imaging with an IVIS Imaging System. Shown is bioluminescent imaging on two sets of *flLucR;NC* littermates with three different *Pak2* genotypes. Mice were injected with *D-luciferin* 6 months (*left* panel) or 7 months (*right*) after IT injection of adeno-Cre virus; mice with excision of *Pak2* show delayed tumor progression as indicated by reduced intensity of luminescent signals. Experiment was repeated four times with similar results.

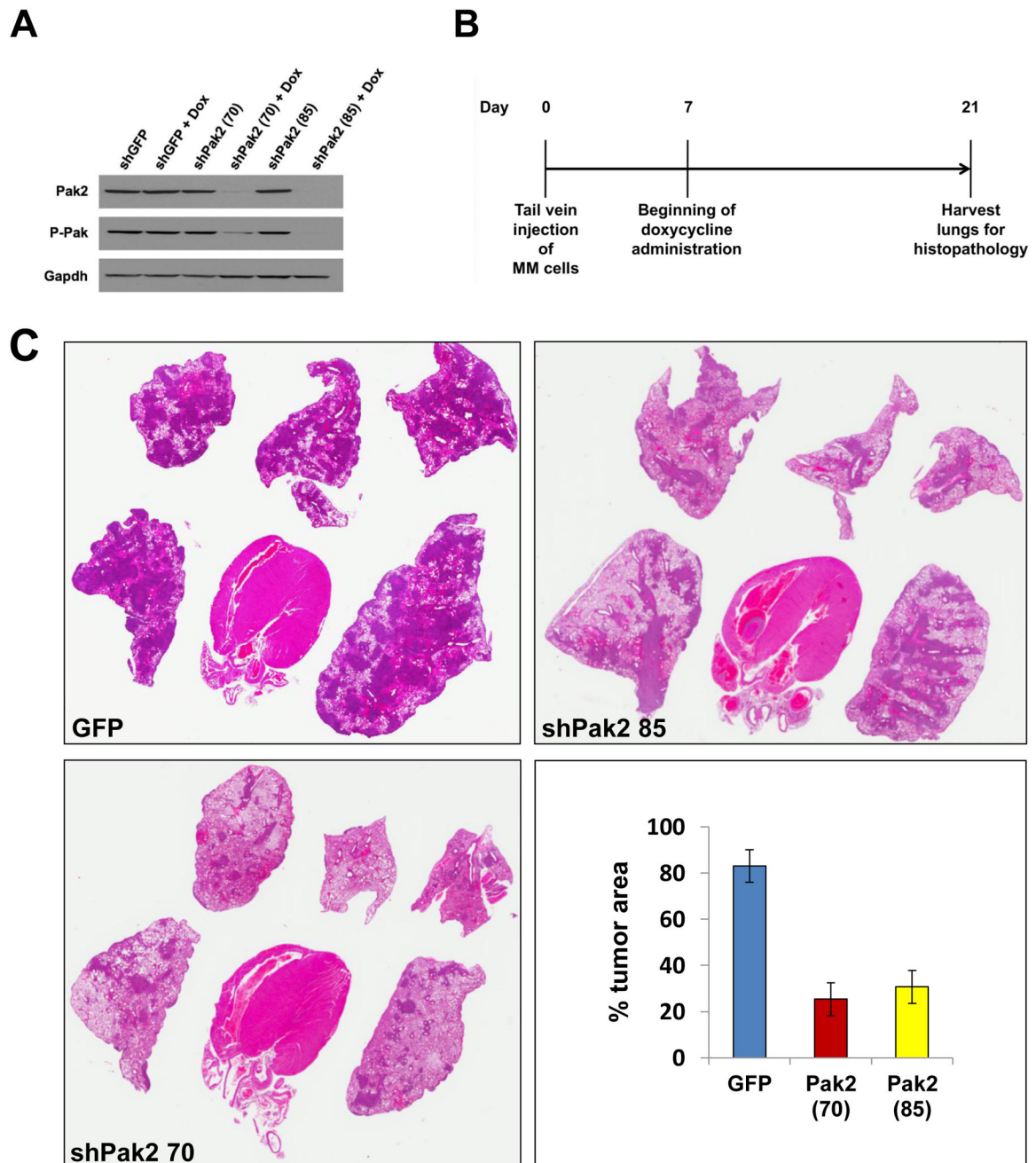


Figure 2.

Knockdown of *Pak2* diminishes metastatic colonization of *Nf2*-deficient mesothelioma cells in the lung. Cell line MM87, which was derived from asbestos-induced mesothelioma from a *Nf2*^{+/-}; *Cdkn2a*^{+/-} mouse, was infected with tet-inducible lentiviruses against *Pak2*. (A) Immunoblot demonstrating expression of Pak2 after knockdown with shRNA. Two clones with robust knockdown of *Pak2* (shPak2 #70 and shPak2 #85) and one clone infected with lentivirus against GFP, used as a control, were selected for tail vein injections into NSG mice. (B) Malignant mesothelioma clones were each injected into the tail vein of three different NSG mice, followed by injection with doxycycline 7 d later and

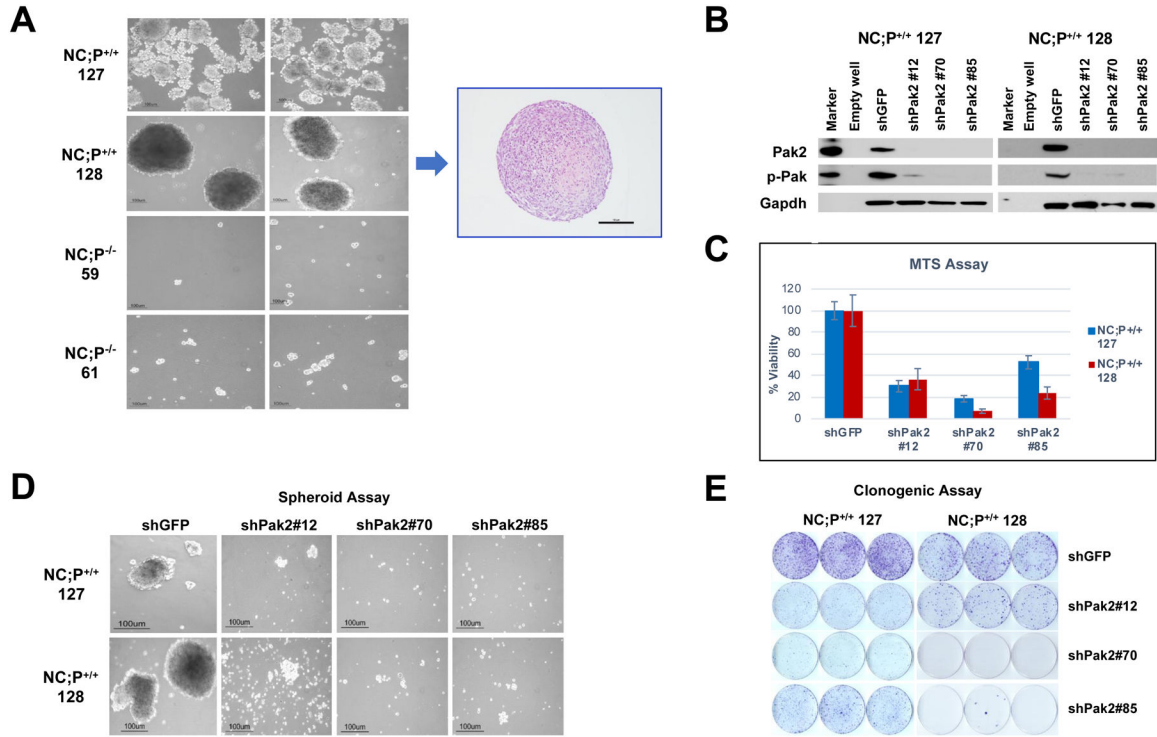
every 2 d thereafter; all animals were sacrificed on d 21, and lungs were collected for histopathological assessment of tumor burden. (C) H&E staining illustrating representative tumor colonization (intensely stained areas) of lungs by MM87 cells expressing shGFP, shPak2 #70 or shPak2 #85. Tumor burden was quantified using an Aperio ScanScope CS2 scanner, as described in the Supplemental Materials and Methods.

Author Manuscript

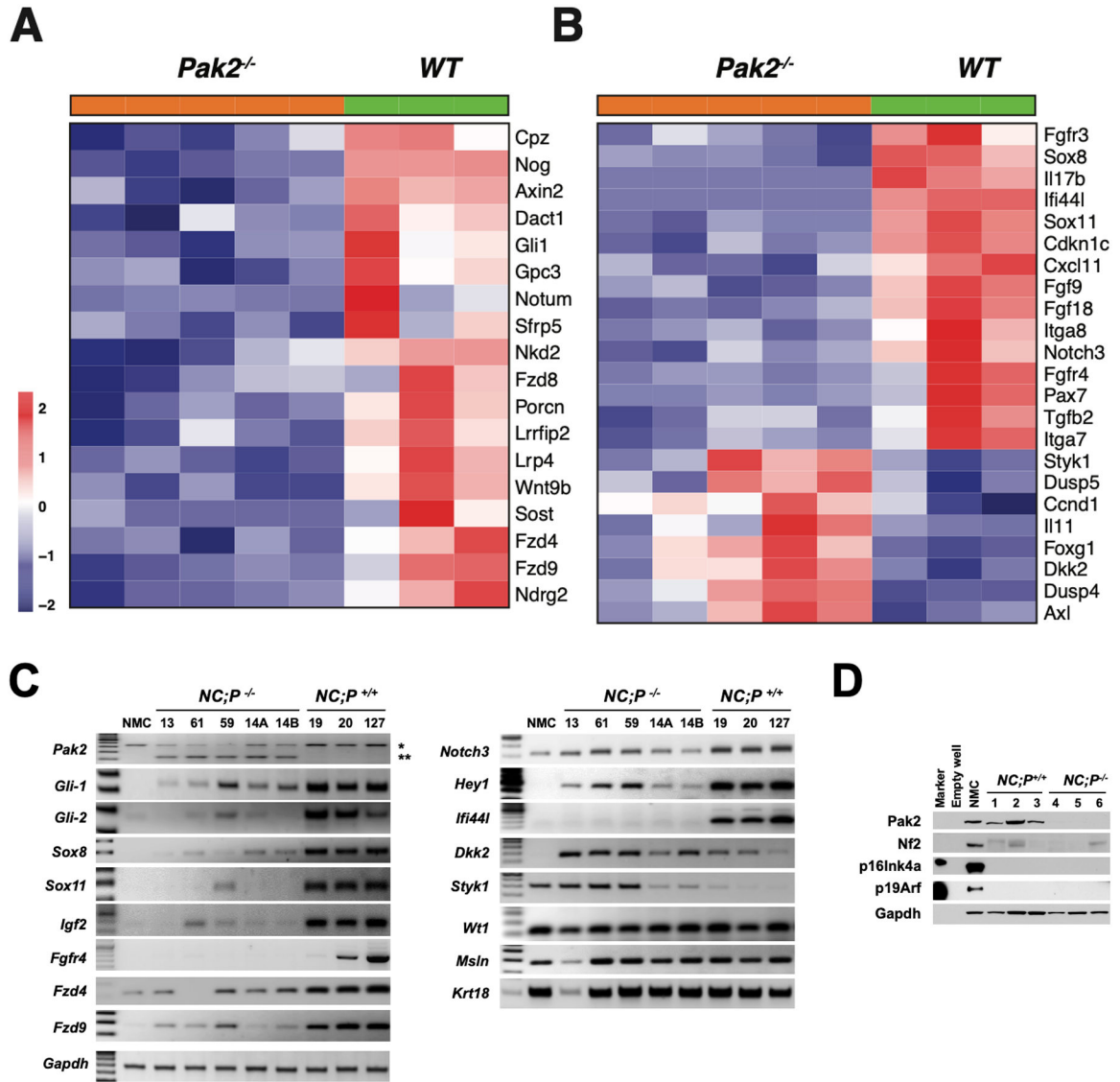
Author Manuscript

Author Manuscript

Author Manuscript

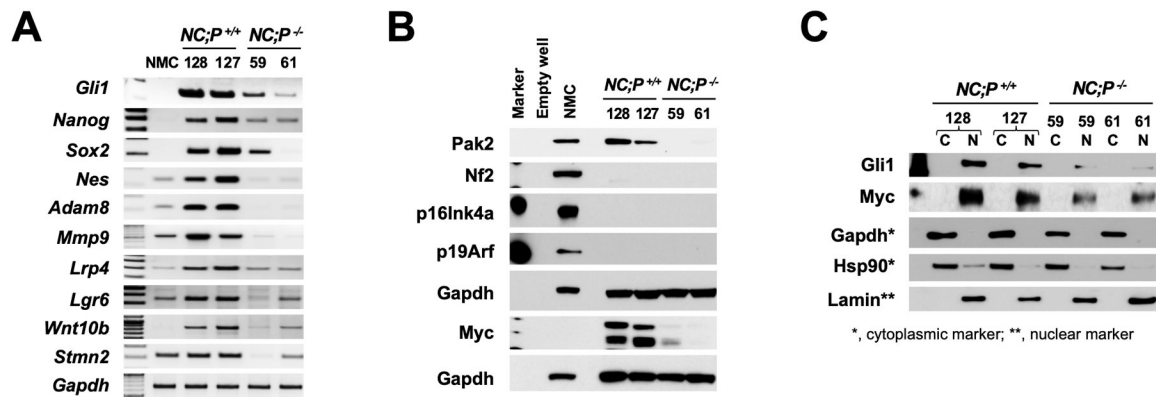
**Figure 3.**

Deletion of *Pak2* results in decreased peritoneal malignant mesothelioma cell viability, clonogenicity, and spheroid formation. (A) *NC;P^{-/-}* mesothelioma cell lines exhibit greatly decreased spheroid formation. Mesothelioma cells were seeded in ultra-low attachment 6-well plates (5,000 cells/well) in stem cell medium, and colonies were photographed after 10 d. H&E staining of a section of typical spheroid from mesothelioma cell line *NC;P^{+/+}* 128 is also shown (A). In other experiments shown, two different *NC;P^{+/+}* mesothelioma cell lines (127, 128) were infected with lentivirus expressing shGFP (control) and three separate shRNA (#12, #70, #85) against *Pak2*. After 4 days, the selection with puromycin was completed, and the cells were collected for immunoblotting and seeded for the experiments described below. (B) Immunoblot analysis demonstrating knockdown of *Pak2* in the two *NC;P^{+/+}* mesothelioma cell lines 4 d after selection with puromycin. Cells with stable knockdown of *Pak2* inhibited mesothelioma cell viability (C), spheroid formation (D), and clonogenicity (E). The MTS assay revealed a significant reduction in cell viability 96 h after seeding with each of the three shPak2 lentiviruses compared to the shGFP lentivirus. The clonogenic assay demonstrated a marked reduction in colony formation 2 weeks after seeding with each of the three shPak2, and knock down of *Pak2* similarly caused a striking decrease in spheroid formation after 10 d of growth *in vitro*.

**Figure 4.**

Heatmaps showing expression patterns of genes in *NC;P*^{+/+} and *NC;P*^{-/-} primary malignant mesotheliomas. Heatmaps depict differentially expressed genes observed in peritoneal malignant mesotheliomas from 3 *NC;P*^{+/+} mice versus 5 peritoneal malignant mesotheliomas from *NC;P*^{-/-} mice. **(A)** Genes involved in Wnt and Hedgehog signaling. **(B)** Differentially expressed genes involved in multiple pathways/functions, including Akt and Notch signaling, cardiac EMT, cell cycling, cancer stem cell (CSC) markers, and integrins. **(C)** Validation of a number of differentially expressed genes by semi-quantitative RT-PCR analysis. *Left*, Down-regulated genes in *NC;P*^{-/-} primary malignant mesotheliomas include genes involved in Hedgehog signaling (*Gli1*, *Gli2*), CSC properties and metastasis (*Sox8*, *Sox11*), Wnt signaling (*Fzd4*, *Fzd9*, *Axin2*), and Akt signaling (*Igf2*, *Fgfr4*). *Right*, Validation of genes involved in Notch signaling (*Notch3*, *Hey1*) and genes involved in tumor reprogramming in *NC;Pak2*^{-/-} mesothelioma cells. Note that *NC;Pak2*^{-/-} cells show downregulation of *Ifi44L*, a tumor suppressor gene that has been implicated in metastasis

and drug resistance by regulating met/Src signaling (49), and upregulation of *Dkk2* and *Styk1*, genes involved in cell proliferation and metastasis. Controls include malignant mesothelioma marker genes *Msln* (mesothelin), *Wt1*, and cytokeratin 18 (*Krt18*). Note that in addition to the mutant deleted *Pak2* allele seen in *NC;P^{-/-}* malignant mesotheliomas, there is also a weak wild type allele due to contaminating stroma in these tumor samples. NMC, normal mesothelial cells; *, wild type *Pak2* allele; **, mutant *Pak2* allele created after adeno-Cre excision of floxed allele. **(D)** Immunoblot analysis confirming the loss of expression of Pak2 (as well as of Nf2, p16Ink4a and p19Arf) in three *NC;P^{-/-}* primary malignant mesotheliomas, whereas Pak2 expression is retained in the three *NC;P^{+/+}* tumors. NMC, normal mesothelial cells.

**Figure 5.**

Loss of Pak2 in peritoneal mesothelioma cell lines results in down regulation of Hedgehog and Wnt signaling as well as CSC and metastasis markers. **(A)** Semi-quantitative PCR analysis of early passage (p. 8) peritoneal *NC;P^{-/-}* and *NC;P^{+/+}* mesothelioma cell lines demonstrating down-regulation of several genes involved in Hedgehog signaling (*Gli1*), CSCs (*Nanog*, *Nes*, *Sox2*), migration/invasion (*Adam8*, *Mmp9*), Wnt signaling (*Lrp4*, *Lgr6*, *Wnt10b*, *Stmn2*). **(B)** Immunoblot analysis of *NC;P^{-/-}* and *NC;P^{+/+}* mesothelioma cell lines demonstrating loss of expression of Pak2, Nf2, p16Ink4a, and p19Arf in all cell lines and loss of expression of Pak2 and the oncoprotein Myc specifically in *NC;P^{-/-}* mesothelioma cells. **(C)** Cell fractionation analysis of peritoneal *NC;P^{-/-}* and *NC;P^{+/+}* mesothelioma cells; immunoblotting demonstrates decreased expression of nuclear localized *Gli1* and *Myc* proteins in *NC;P^{-/-}* cell lines 59 and 61. C, cytoplasmic lysate; N, nuclear lysate.

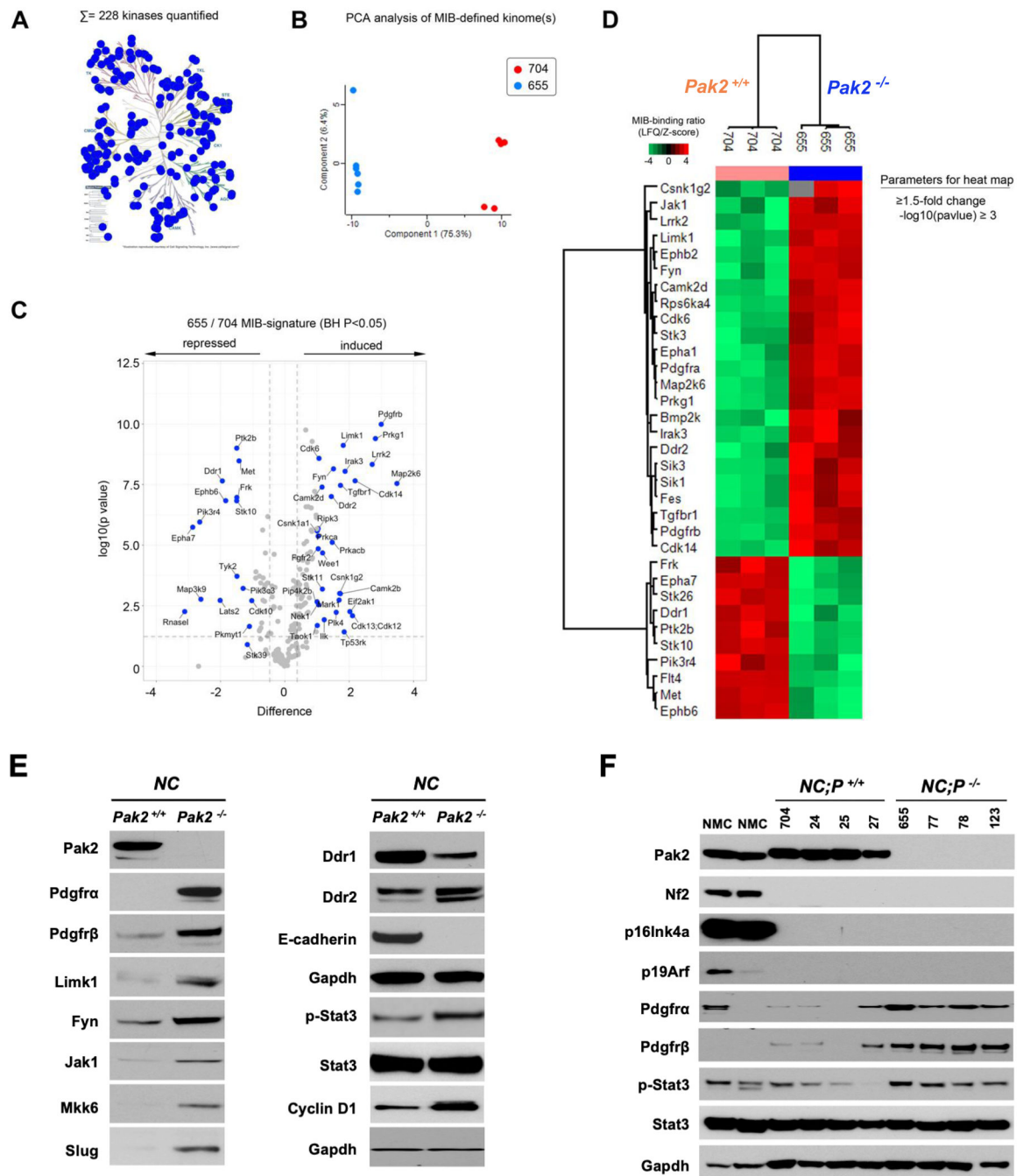


Figure 6. Kinome profiling of *NC;P^{-/-}* pleural mesothelioma cells and *NC;P^{+/+}* mesothelioma cells. Early passage pleural mesothelioma cell cultures were derived from tumors observed in *Nf2^{fl/fl};Cdkn2a^{fl/fl}* and *Nf2^{fl/fl};Cdkn2a^{fl/fl};Pak2^{fl/fl}* mice injected IT with adeno-Cre virus. (A) Kinome activity as measure by MIBs. (B) PCA analysis, showing differential kinome profiles. (C) Volcano plot depicts kinases exhibiting induced or repressed MIB binding in cells with knockout of Pak2. (D) Heat-map depicts statistical changes in kinase levels between one *NC;P^{-/-}* mesothelioma cell line and one *NC;P^{+/+}* mesothelioma cell line,

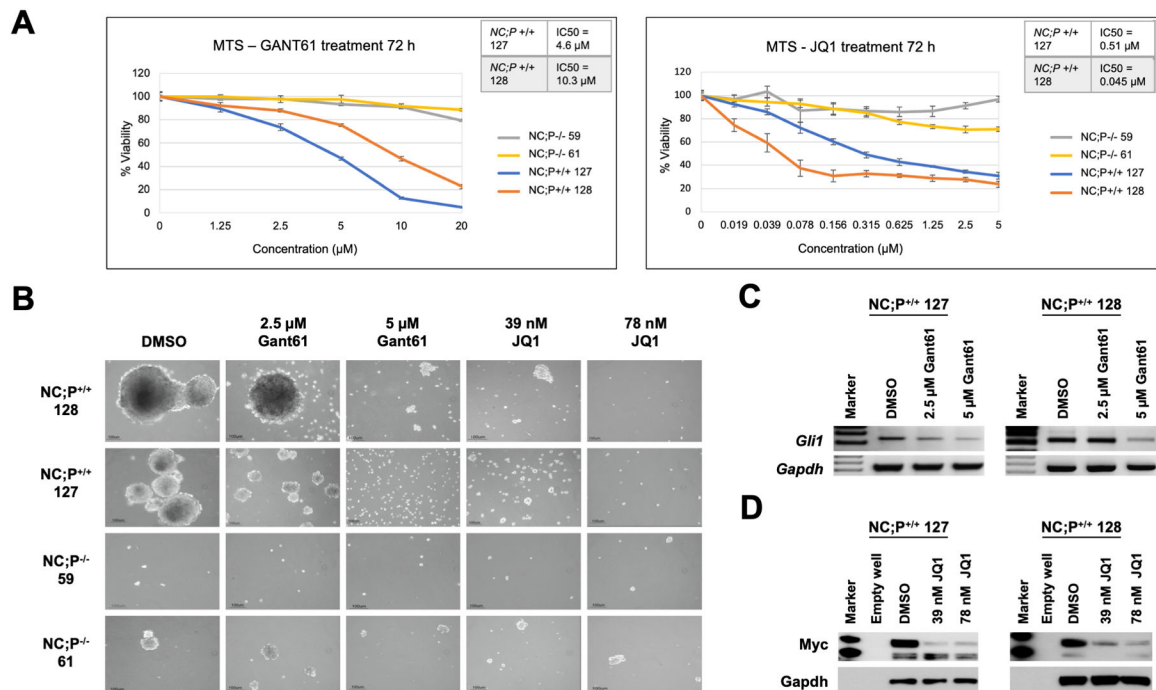
with experiment performed in triplicate. (E) Immunoblot confirmation of expression changes in selected kinases in these two cell lines. (F) Immunoblot analysis confirming consistently up-regulated expression of Pdgfr α , Pdgfr β , and p-Stat3 in *NC;P^{-/-}* versus *NC;P^{+/+}* mesothelioma cell lines.

Author Manuscript

Author Manuscript

Author Manuscript

Author Manuscript

**Figure 7.**

Targeting of Gli1 or Myc each inhibits cell viability and spheroid formation in *NC;P^{+/+}* mesothelioma cells. **(A)** Early passage *NC;P^{-/-}* and *NC;P^{+/+}* peritoneal mesothelioma cell lines were seeded in 96-well plates (2,500 cells/well) and treated with indicated concentrations of GANT61 or JQ1 for 72 h in medium supplemented with 2.5% FBS for GANT61 treatment and 10% FBS for JQ1. MTS assays show significant decreases in cell viability in *NC;P^{+/+}* cells compared to *NC;P^{-/-}* cells at increasing concentrations of GANT61 and JQ1. IC50 values for the two *NC;P^{+/+}* cell lines were determined using GraphPad Prism. IC50's were not determined for the *NC;P^{-/-}* cell lines, as these cells were very insensitive to GANT61 and JQ1 due to their low expression of Gli1 and Myc, respectively. **(B)** Morphological appearance of spheroids in presence or absence of GANT61 and JQ1. *NC;P^{-/-}* and *NC;P^{+/+}* cells were seeded in 6-well plates (5,000 cells/well) in stem cell medium and treated with GANT61 (2.5 and 5 μM) or JQ1 (39 and 78 nM), and cells were photographed after 10 d. Both GANT61 (at 5 μM) and JQ1 (both at 39 and 78 nM) markedly inhibited spheroid formation in *NC;P^{+/+}* cells compared to cells cultured in medium containing vehicle (DMSO). In contrast, neither drug had much effect on *NC;P^{-/-}* cells. **(C)** Semi-quantitative PCR analysis was performed on *NC;P^{+/+}* cell lines treated as above, and after treatment with drugs for 72 h. RNA was extracted with TRIzol and semi-quantitative PCR was performed. **(D)** Immunoblot analysis of *NC;P^{+/+}* cells treated with different concentrations of JQ1. Cells were seeded in 6-well plates, treated with JQ1 for 72 h, lysed, and subjected to immunoblot analysis, which demonstrates inhibition of Myc expression by the drug treatment.